Comparative Study on Estimating the External Torque of Flexible Robot Driven by Series Elastic Actuators

Liu Shenghong [1], Wang Gao [1], Liu Ning [1], and Min Feiyan [1,*]

[1]School of Information Science and technology, Jinan University, Guangzhou 510632, China

*Correspondence

E-mail: liushenghong@stu2018.jnu.edu.cn

Abstract. Accurate and fast estimation of external torque applied to the robot body directly determines the final performance of force control for flexible robot driven by series elastic actuators. The external torque estimation based on dynamics model requires the state information of robot link side, including angle, angular velocity and angular acceleration. Due to the noise and uncertainty of angular acceleration signal obtained by discrete differentiation of the angle, most methods of external torque estimation take the method of avoiding acceleration calculation. In this paper, an extended Kalman filter (EKF) algorithm is used to fuse the information of the photoelectric encoder and accelerometer to obtain the accurate link side angular acceleration signal, which is used to directly estimate (DE) the external torque based on the dynamic model. The results show that the momentum observer (MOB) has the same effect as reaction torque observer (RTOB), and the direct estimation method of precise acceleration signal has high accuracy and wide band. Also, the experiments in turn demonstrate the accuracy of the angular acceleration signal obtained by the EKF fusion.

Keywords: force estimation, momentum observer, reaction torque observer, accelerometer calibration, extended Kalman filter

1. Introduction

In recent years, there has been a surge of interest in flexible joint robots with inherent adaptations. Unlike rigid robots, the drive joints of flexible joint robots have elastic elements between the motor side and the link side, introducing low output impedance, force sensing, passive mechanical energy storage, and increasing peak output power [1]. In addition, the inherent flexibility of the elastomer can soften the impact, protect the drive mechanism, and improve the safety of human-machine interaction. Because of these characteristics, flexible joint robots are widely used in the field of force control, such as exoskeleton robots, industrial flexible machining and assembly, medical surgery, etc., which physically interact with their surroundings [2–4].

In robot force control, the external force applied to the robot body can be transformed into the external torque applied to each joint by the Jacobian matrix of force. Dynamic, rapid, and accurate identification of the external torque applied to each joint is essential for achieving accurate and stable force control.

The most direct method to measure the external torque is to mount force/torque sensors in robot joints or on the robot surface. However, there are many obvious drawbacks to this simple method. For example, the precise installation of sensors increases the mechanical, electrical and software design complexity of the entire robot equipment and increases the cost of robot design and assembly. Also, the position where the force acts becomes limited, which limits the robot's use conditions, making it difficult to be applied universally to different types of robots. In addition, the force output signal needs to be filtered and amplified to be transformed into recognizable digital signals, and there are many uncertain perturbations and environmental changes (such as environmental temperature change and external electromagnetic interference), which may affect the accuracy and reliability and even seriously affect the normal operation of the force sensor.

Most of the robot external force estimation studies are achieved indirectly by obtaining robot state information, including angle, angular velocity, and angular acceleration, combined with a dynamics model. Since the robotic arm joint acceleration is usually not available by direct measurement and the acceleration signal obtained by direct discrete quadratic differentiation of the joint angle may be entrained with uncertain perturbations, conventional methods usually use different techniques to avoid the direct use of the acceleration signal. De Luca et al.[5] proposed a method based on generalized momentum, which avoids the use of joint acceleration in their research on detecting and isolating robot executive structural faults. And this method is widely used in robot external force estimation [6, 7]. Furthermore, in order to avoid direct acquisition of the robot joint acceleration, Ohnishi et al. used the method of constructing the dynamic model in the mathematical form of the Laplace domain to estimate the external torque for the force control feedback loop [8, 9].

With the further study of accelerometer angular veloc-

ity measurement [10], the method of accelerometer direct measurement of the angular acceleration of joint is introduced into the robot control process [11, 12].

This paper does not consider the control of the motor side of the flexible joint, and mainly uses the dynamic model of the link side to analyze the performance of the traditional method (avoid using angular acceleration) and the direct calculation method based on the dynamic model (obtain precise angular acceleration by accelerometer) in obtaining the external torque. In order to obtain accurate angular acceleration information, the initial relative position and orientation of accelerometer and robot are calibrated, and then the data of accelerometer and photoencoder are fused with the extended Kalman filter algorithm.

This paper consists of five sections. The first section introduces the research background of this paper. The second part mainly introduces the dynamic model of flexible robot and three typical external torque estimation methods. All three methods require information about the state of the robot's connector, such as joint speed and acceleration. Therefore, in the third section, the method of obtaining joint velocity and angular acceleration is introduced. It is worth noting that the angle signal of the photoencoder is merged with acceleration signal linear acceleration signal of the accelerometer by using Kalman to obtain the status information of the link side. The experimental part is presented in the fourth section, and the analysis and conclusion are drawn in the fifth section.

2. External torque estimation methods

The dynamic model of a flexible robot with series elastic actuators as driving joints can be written as:

$$\boldsymbol{M}(\boldsymbol{q})\ddot{\boldsymbol{q}}+\boldsymbol{C}(\boldsymbol{q},\dot{\boldsymbol{q}})\dot{\boldsymbol{q}}+\boldsymbol{g}(\boldsymbol{q})+\boldsymbol{\tau}_{ext}=\boldsymbol{\tau}_{sp} \quad (1)$$

$$\boldsymbol{J}_m\ddot{\boldsymbol{\theta}}+\boldsymbol{\tau}_{fric}+\boldsymbol{\tau}_{sp}=\boldsymbol{\tau}_m \quad (2)$$

$$\boldsymbol{\tau}_{sp}=\boldsymbol{K}_{sp}(\boldsymbol{\theta}-\boldsymbol{q}) \quad (3)$$

where $\boldsymbol{M}(\boldsymbol{q})$ denotes the inertia matrix, $\boldsymbol{C}(\boldsymbol{q},\dot{\boldsymbol{q}})$ denotes the centripetal and Coriolis matrix and $\boldsymbol{g}(\boldsymbol{q})$ denotes the gravity vector. $\boldsymbol{\theta}$ and $\boldsymbol{q}$ are respectively the motor and link angles. $\boldsymbol{\tau}_{ext}$ and $\boldsymbol{\tau}_{sp}$ are the external torque applied to the robot link and the torque applied by the elastic joint deformation respectively. $\boldsymbol{\tau}_m$ and $\boldsymbol{\tau}_{fric}$ denotes motor torque acting on the motor inertia $\boldsymbol{J}_m$ and friction torque. $\boldsymbol{K}_{sp}$ denotes the Hooke coefficient of the torsion spring in the joint of the series elastic actuator.

Hooke coefficient of torsion spring is determined after system identification. Photoelectric encoders are installed at both ends of the serial elastic driver (motor side and link side) to collect position information, so the driving torque of the link can be calculated by the deformation of the torsion spring.

2.1. Momentum observer

In the process of robot movement, if the external environment and the robot interact with force/torque, the robot's momentum often changes significantly. Therefore, the external force/torque can be estimated by observing the real-time change of the robot's momentum.

Robot generalized momentum is defined by formula(4).

$$\boldsymbol{L}=\boldsymbol{M}(\boldsymbol{q})\dot{\boldsymbol{q}} \quad (4)$$

According to classical robot dynamics, matrix $\dot{\boldsymbol{M}}(\boldsymbol{q})-2\boldsymbol{C}(\boldsymbol{q},\dot{\boldsymbol{q}})$ is an antisymmetric matrix, so $\dot{\boldsymbol{M}}(\boldsymbol{q})-2\boldsymbol{C}(\boldsymbol{q},\dot{\boldsymbol{q}})=2\boldsymbol{C}^T(\boldsymbol{q},\dot{\boldsymbol{q}})-\dot{\boldsymbol{M}}^T(\boldsymbol{q})$. Since the inertia matrix of the robot is a symmetric positive matrix, the above dequation can be transformed into

$$\dot{\boldsymbol{M}}(\boldsymbol{q})=\boldsymbol{C}(\boldsymbol{q},\dot{\boldsymbol{q}})+\boldsymbol{C}^T(\boldsymbol{q},\dot{\boldsymbol{q}}) \quad (5)$$

Differentiate the generalized momentum of the robot and then substitute formula(5) and the dynamics equation of the link side(1) into it, $\dot{\boldsymbol{L}}$ can be written as

$$\begin{aligned}\dot{\boldsymbol{L}}&=(\boldsymbol{C}(\boldsymbol{q},\dot{\boldsymbol{q}})+\boldsymbol{C}^T(\boldsymbol{q},\dot{\boldsymbol{q}}))\dot{\boldsymbol{q}}+\boldsymbol{M}(\boldsymbol{q})\ddot{\boldsymbol{q}}\\&=\boldsymbol{\tau}_{sp}-\boldsymbol{\tau}_{ext}-[\boldsymbol{C}^T(\boldsymbol{q},\dot{\boldsymbol{q}})\dot{\boldsymbol{q}}+\boldsymbol{g}(\boldsymbol{q})]\end{aligned} \quad (6)$$

As can be seen from equation(6), momentum and external torque are decoupled. Therefore, the momentum observer is designed according to the formula $\boldsymbol{r}(t)=Ko[\int_0^t(\boldsymbol{\tau}_{sp}+\boldsymbol{C}^T(\boldsymbol{q},\dot{\boldsymbol{q}})\dot{\boldsymbol{q}}-\boldsymbol{g}(\boldsymbol{q})-\boldsymbol{r})dt-(\boldsymbol{L}(t)-\boldsymbol{L}(0))]$ to estimate external torque, as shown in **Fig**.**2**. The dynamic form of $\boldsymbol{r}$ can be written as $\dot{\boldsymbol{r}}=Ko(-\boldsymbol{r}+\boldsymbol{\tau}_{ext})$. It can described as a formula $\boldsymbol{r}=\frac{Ko}{s+Ko}\boldsymbol{\tau}_{ext}$ in the Laplace domain. When $Ko\to\infty,\boldsymbol{r}\approx\boldsymbol{\tau}_{ext}$, that is, the torque observed by MOB is the filtering result of the actual external torque.

2.2. Reaction torque observer

The Reaction Torque Observer, as shown in **Fig**.**1**(**b**), is mainly obtained by deforming the dynamic equation of the link side in the Laplace transform domain. The external torque can be estimated only by observing the driving torque and angular velocity, which avoids the requirement of angular acceleration in the dynamic equation, as shown in formula (7).

$$\begin{aligned}\hat{\boldsymbol{\tau}}_{ext}=&\frac{g_{ob}}{s+g_{ob}}[\boldsymbol{K}_{sp}(\boldsymbol{\theta}-\boldsymbol{q})-\boldsymbol{g}(\boldsymbol{q})-g_{ob}\boldsymbol{M}(\boldsymbol{q})\dot{\boldsymbol{q}}]\\&-g_{ob}\boldsymbol{M}(\boldsymbol{q})\dot{\boldsymbol{q}}\end{aligned} \quad (7)$$

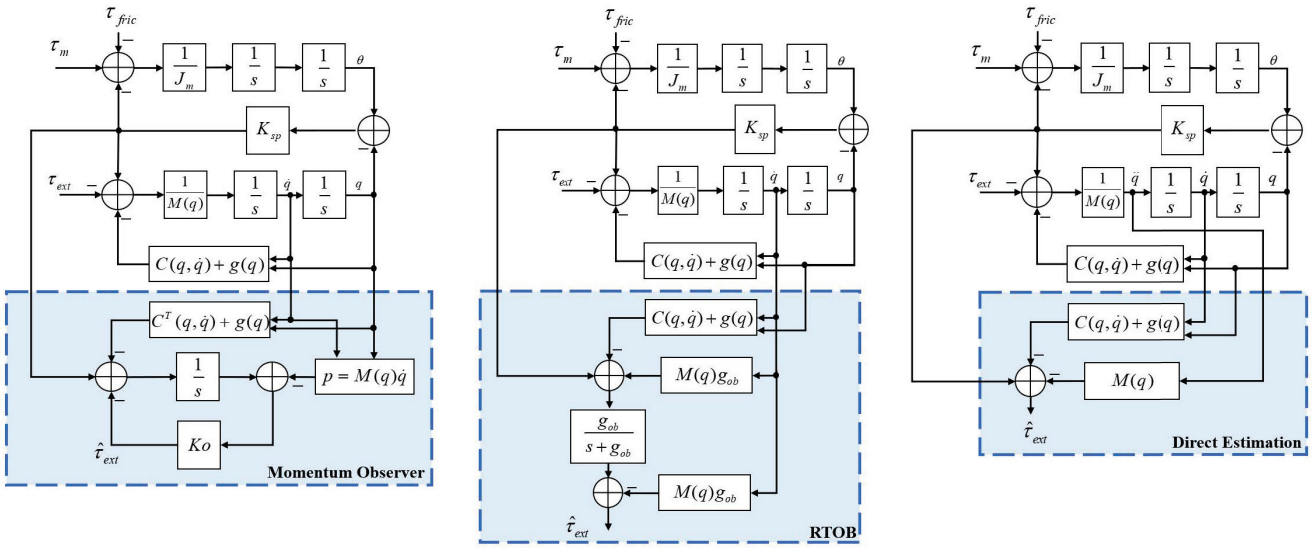
where g_{ob} denotes the observer bandwidth. The purpose is to filter out the sensor measurement noise and the effect of quantization noise on the system.

2.3. Direct estimation based on dynamics model

Based on the system dynamics model, the external force is directly calculated from the dynamics equation (1) of the link side of robot, as shown in **Fig**.**1**(**c**).

$$\boldsymbol{\tau}_{ext}=\boldsymbol{K}_{sp}(\boldsymbol{\theta}-\boldsymbol{q})-\boldsymbol{M}(\boldsymbol{q})\ddot{\boldsymbol{q}}-\boldsymbol{C}(\boldsymbol{q},\dot{\boldsymbol{q}})\dot{\boldsymbol{q}}-\boldsymbol{g}(\boldsymbol{q}) \quad (8)$$

The robot's driving torque and real-time joint angle need to be observed in these three force estimation methods. The difference is that MOB and RTOB only need to observe the real-time angular velocity of the link side, while DE needs to obtain the real-time angular acceleration.



(a) Momentum Observer (b) Reaction Torque Observer (c) Direct Estimation

Fig. 1. External torque estimation methods

3. State information acquisition of robot link side

In the traditional robot control system, the angle of the robot SEA joint is collected by adding photoelectric encoders at two ends of the joint. To obtain the link side angular velocity $\dot{\boldsymbol{q}}$ and angular acceleration $\ddot{\boldsymbol{q}}$, the first and second differential of the angle returned by the photoelectric encoder will amplify the quantization noise of the sensor and make the signal unusable. Therefore, differential results are generally filtered, but the introduction of filtering will lead to the delay of robot link state information while filtering out sensor measurement noise and reducing the real-time and even stability of the control system.

To obtain the angular acceleration signal of the link, accelerometers are mounted on each link of robot. The angular acceleration is obtained by fusing the linear acceleration signal returned by the accelerometer and the position signal produced by the photoelectric encoder with the extended Kalman filter.

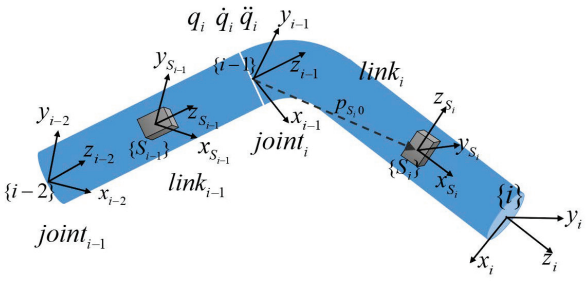


Fig. 2. Nonlinear relationship between sensors and links

3.1. Accelerometer sensor calibration

After the accelerometer is installed on the link i, the initial relative position $\boldsymbol{p}_{S0}$ and the orientation $\boldsymbol{R}_{S0}$ between the accelerometer and joint i need to be determined. In the robot control system, the standard DH modeling method is adopted; that is, the last joint of the link is taken as its fixed coordinate frame, as shown in **Fig.2**.

The initial relative position and the orientation metioned above can use four parameters $\theta_S, d_S, r_S, \alpha_S$ to describe, as

$$\begin{aligned} T_{S0} &= Rotz(\theta_S)Transz(d_S)Transx(r_S)Rotz(\alpha_S) \\ &= \begin{bmatrix} \boldsymbol{R}_{S0} & \boldsymbol{p}_{S0} \\ \boldsymbol{0} & 1 \end{bmatrix} \end{aligned} \tag{9}$$

The robot in this paper is joint type robot, so ${}^{i-1}\boldsymbol{\omega}_i = \begin{bmatrix} 0 & 0 & \dot{q}_i \end{bmatrix}^T$. The linear velocity of the sensor caused by the rotation of joint i can be expressed as

$$\begin{aligned} {}^{i-1}\boldsymbol{v}_S &= {}^{i-1}\boldsymbol{\omega}_i \times {}^{i-1}\boldsymbol{p}_S = {}^{i-1}\boldsymbol{\omega}_i \times [\boldsymbol{Rz}(q_i)\boldsymbol{p}_{S0}] \\ &= {}^{i-1}\boldsymbol{J}_S\dot{q}_i \end{aligned} \tag{10}$$

Further, taking the derivative of equation (10), the linear acceleration of the sensor ${}^{i-1}a_S$ caused by the rotation of joint i can be expressed as

$${}^{i-1}\boldsymbol{a}_S = {}^{i-1}\dot{\boldsymbol{v}}_S = {}^{i-1}\boldsymbol{J}_S\ddot{q}_i + {}^{i-1}\dot{\boldsymbol{J}}_S\dot{q}_i \tag{11}$$

Let ${}^{i-1}\boldsymbol{R}_w(\boldsymbol{q})$ and ${}^{w}\boldsymbol{R}_{i-1}(\boldsymbol{q})$ represent the orientation from the world frame {w} to the fixed frame {i-1} of joint i. In the calibration process, only the current joint i is rotated and the other joints are in the zero position, so $\boldsymbol{q} = \boldsymbol{0}$.

In addition, the frame {i-1} is fixed with respect to the world frame {w} during calibration. The accelerometer frame {S} is affected by joint rotation q_i. Considering the effect of the acceleration of gravity ${}^{w}\boldsymbol{g}$, the deviation of the accelerometer and the conversion relationship be-

tween reference frame, the linear acceleration relative to the accelerometer frame can be written as

$$\begin{aligned} {}^{S}\boldsymbol{a}_S &= {}^{S}\boldsymbol{R}_{i-1}(q_i)\,{}^{i-1}\boldsymbol{R}_w(\boldsymbol{q})\,{}^{w}\boldsymbol{R}_{i-1}(\boldsymbol{q})({}^{i-1}\boldsymbol{a}_S + {}^{w}\boldsymbol{g}) + \boldsymbol{b} \\ &= {}^{S}\boldsymbol{R}_{i-1}(q_i)\,{}^{i-1}\boldsymbol{R}_w(\boldsymbol{0})\,{}^{w}\boldsymbol{R}_{i-1}(\boldsymbol{0})({}^{i-1}\boldsymbol{a}_S + {}^{w}\boldsymbol{g}) + \boldsymbol{b} \end{aligned} \quad (12)$$

$\dot{q}_i$ and $\ddot{q}_i$ can be obtained by off-line processing of angle q_i collected from the encoder, which are used as input data for calibration parameter identification, and 3-dimension linear acceleration obtained from the accelerometer is used as output data. The identification algorithm can obtain the accelerometer sensor's initial position and orientation relative to the joint frame {i-1}, including seven parameters.

3.2. System state acquisition based on extended Kalman filter

Because of various uncertainty factors in the system, such as imperfect mathematical models, difficult to control and model system disturbance, sensor measurement noise, etc., the state of the system is often inaccurate. The Kalman filter algorithm solves this problem effectively and is widely used in motion control systems. The Kalman filter algorithm can estimate the process state of the system effectively by minimizing the squared mean of errors. It can effectively filter out the noise of measurement systems, correct the state of the system and reduce the influence of system uncertainty.

The dynamic state model of the system is

$$\frac{d}{dt}\begin{bmatrix} q_i \\ \dot{q}_i \\ \ddot{q}_i \\ \dddot{q}_i \end{bmatrix} = \begin{bmatrix} 0 & 1 & 0 & 0 \\ 0 & 0 & 1 & 0 \\ 0 & 0 & 0 & 1 \\ 0 & 0 & 0 & 0 \end{bmatrix}\begin{bmatrix} q_i \\ \dot{q}_i \\ \ddot{q}_i \\ \dddot{q}_i \end{bmatrix} + \boldsymbol{w} \quad . \; . \; . \; (13)$$

In order to improve the result of state estimation, the measurement equation combines the measurement values of the photoelectric encoder and the accelerometer. Note the system variable as $\boldsymbol{x} = \begin{bmatrix} q_i & \dot{q}_i & \ddot{q}_i & \dddot{q}_i \end{bmatrix}^T$. The system measurement model is

$$\boldsymbol{z} = \begin{bmatrix} q_i \\ {}^{S_i}\boldsymbol{a}_{S_i}(q_i, \dot{q}_i, \ddot{q}_i) \end{bmatrix} + \boldsymbol{v} = h(\boldsymbol{x}) + \boldsymbol{v} \quad . \; . \; . \; . \; . \; (14)$$

where $\boldsymbol{w}$ and $\boldsymbol{v}$ are system process noise and measurement noise, respectively. ${}^{S_i}\boldsymbol{a}_{S_i}(q_i, \dot{q}_i, \ddot{q}_i)$ is a nonlinear relationship $h(\cdot)$, as shown in **Fig.2**.

The linear acceleration directly returned from the accelerometer is relative to the frame $\{S_i\}$, and can be converted to the fixed frame {i-1} of the joint i through the relationship ${}^{S_i}\boldsymbol{a}_{S_i} = {}^{S}\boldsymbol{R}_{i-1}(q_i)\,{}^{i-1}\boldsymbol{a}_{S_i}$.

${}^{i-1}\boldsymbol{a}_{S_i}$ can be split into centripetal acceleration, centrifugal acceleration caused by the rotation of joint i, and linear acceleration synthesized by previous joint motion ${}^{i-1}\boldsymbol{a}_{offset}$ (which includes gravitational acceleration).

$$\begin{cases} {}^{i-1}\boldsymbol{a}_{S_i} = {}^{i-1}\dot{\boldsymbol{\omega}}_i \times {}^{i-1}\boldsymbol{p}_{S_i} \\ \qquad + {}^{i-1}\boldsymbol{\omega}_i \times {}^{i-1}\boldsymbol{\omega}_i \times {}^{i-1}\boldsymbol{p}_{S_i} + {}^{i-1}\boldsymbol{a}_{offset} \\ {}^{i-1}\boldsymbol{p}_{S_i} = \boldsymbol{Rz}(q_i)\boldsymbol{p}_{S_i0} \\ {}^{i-1}\boldsymbol{\omega}_i = {}^{i-1}\boldsymbol{\omega}_{i-1} + \begin{bmatrix} 0 & 0 & \dot{q}_i \end{bmatrix}^T \\ {}^{i-1}\dot{\boldsymbol{\omega}}_i = {}^{i-1}\dot{\boldsymbol{\omega}}_{i-1} + \begin{bmatrix} 0 & 0 & \ddot{q}_i \end{bmatrix}^T \end{cases} \quad (15)$$

Linear acceleration ${}^{i-1}\boldsymbol{a}_{offset}$ is the representation on the frame {i} of the linear acceleration synthesized from link 0 to link i-1 during the movement process, which can be obtained by converting the measurement result returned by the accelerometer fixed on the link i-1 to the coordinate system {i-1}, as follows.

$$\begin{aligned} &{}^{i-1}\boldsymbol{a}_{offset} = \\ &{}^{i-1}\boldsymbol{R}_{i-2}\,{}^{i-2}\boldsymbol{R}_{S_{i-1}}\,{}^{S_{i-1}}\boldsymbol{a}_{S_{i-1}} + \\ &{}^{i-2}\dot{\boldsymbol{\omega}}_{i-1} \times ({}^{i-2}\boldsymbol{p}_{i-1} - {}^{i-2}\boldsymbol{p}_{S_{i-1}}) + \\ &{}^{i-2}\boldsymbol{\omega}_{i-1} \times {}^{i-2}\boldsymbol{\omega}_{i-1} \times ({}^{i-2}\boldsymbol{p}_{i-1} - {}^{i-2}\boldsymbol{p}_{S_{i-1}}) \end{aligned} \quad . \; . \; . \; (16)$$

Where, ${}^{i-1}\boldsymbol{R}_{i-2}$ and ${}^{i-2}\boldsymbol{p}_{i-1}$ are the relationship determined by the robot positive kinematics. ${}^{i-2}\boldsymbol{p}_{S_{i-1}}$ and ${}^{i-2}\boldsymbol{R}_{S_{i-1}}$ are position and orientation determined by the accelerometer calibration. ${}^{i-1}\boldsymbol{\omega}_i, {}^{i-1}\dot{\boldsymbol{\omega}}_i, {}^{i-2}\boldsymbol{\omega}_{i-1}, {}^{i-2}\dot{\boldsymbol{\omega}}_{i-1}$ are obtained by recursive transfer between between the mutually connected links.

The general form of KF is suitable for the linearity of the system state equation and measurement equation. Due to the nonlinearity of the system measurement equation in this paper, the EKF is used for sensor data fusion.

4. Experiment and discussion

4.1. Experimental setup

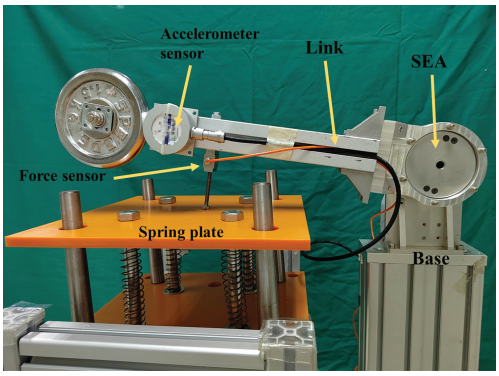


Fig. 3. The experimental setup of the flexible robot system

To facilitate the comparison of different performances of external force estimation, series elastic actuators are used as the single DOF robot driving joints, as shown in **Fig.3**. In the experiment, a 13-bit photoelectric encoder is installed on the motor side to collect motor position information for motor control; a 16-bit photoelectric encoder is installed on the link side to manage the position information of the link. The angular acceleration of the link side is measured by directly mounting a three-dimensional accelerometer on the link side as an additional input for EKF data fusion. Between the robot link and the external environment (spring plate), a force sensor is installed as an intermediate medium to directly measure the external moment acting on the link as a standard reference for estimating external forces by different methods.

4.2. Experimental results

In this work, by controlling the motor to make the robot link move and interact with the external environment (spring plate), we study the different effects of methods proposed in Section 3 on detecting external forces during the entire interaction process.

The entire interaction process is divided into seven stages. Stage 1: The link is stationary at an angle close to the spring plate but not in contact. Stage 2: The link starts to move until it contacts the spring plate. Stage 3: The link presses down on the spring plate. Stage 4: The link and spring plate remain relatively stationary. Stage 5: The link leaves the spring plate until there is no contact with the spring plate. Stage 6: After leaving the spring plate, the spring plate is free to vibrate due to the joint's flexibility. Stage 7: The link is stationary at the starting angle.

As shown in **Fig**.**4**, the state information of the link is recorded, including the angle, angular velocity, and angular acceleration of the link side. "EKF" represents the link status information calculated in real time by fusing sensor datas using the extended Kalman filter. "Differentiation + Filtering" represents the direct differencing and filtering of the position signals collected in real time on the control system. "Offline smooth" denotes the result of offline differencing and sliding window averaging of the joint link side angle signal returned by the photoelectric encoder. The mean smoothing of the signal leads to the loss of the high frequency component of the state information, but does not cause a delay in the signal, and it is used for comparative reference of the robot system real-time status information.

It can be seen that the angular velocity and angular acceleration information obtained by the commonly used method of differential post-filtering of the position will cause the delay of the signal, and the high-frequency components of the signal will be filtered out by the filter, resulting in a relatively low upper limit of the system bandwidth. However, by merging the accelerometer signal with the photoelectric encoder signal through the EKF, a velocity signal and an acceleration signal with almost no delay and a sufficiently wide bandwidth can be obtained. For example, at 1.7-2.2s and 8.4-8.7s, EKF can detect fast-changing high-frequency acceleration signals. In other cases, the results of EKF are similar to those of offline sliding smoothing, which proves the accuracy of the results obtained by EKF fusion of two sensor signals.

In the case of the MOB and the RTOB for external torque estimation, the angular velocity signal input to the observer is obtained by direct differential plus filtering of the position signal returned from the photoelectric encoder, because these two methods are proposed based on the unavailability of the angular acceleration signal. The model-based direct torque estimation method uses the angular acceleration signal estimated by EKF directly.The external force estimation results of the three methods are shown in **Fig**.**5**. The outcomes measured by the force sensor are also displayed.

Among them, the most significant difference lies in stage 3 (pressing process), and stage 6 (free oscillation of the link), and the external force estimation results of these two stages are displayed separately in **Fig**.**5**(**b**) and **Fig**.**5**(**c**). Stage 3 is the process in which the link presses the spring plate. The external torque acting on the link in this process changes rapidly and can reflect the following rapidity of the external toruqe estimation. Stage 6 is the free oscillating motion of the link caused by the joint flexibility after the link leaves the spring plate, in which the link is not subject to external torque and the external torque estimation result should be zero. It can be seen that the results of MOB and RTOB are the same. The reason is that the mathematical models of the two methods are essentially the same. The results obtained by both methods have a more pronounced delay compared to the reference value (measured directly by the force sensor), the external torque follows more slowly, and the presence of the system state delay leads to the detection of large external torque fluctuations even when the link is not subjected to external torque. However, the direct estimation method is characterized by high sensitivity and precision in external torque estimation.

5. Conclusion

This paper analyzes three methods for robot external torque estimation, including momentum observer, reaction torque observer, and direct computations based on model dynamics. The EKF method is used to fuse the three-dimensional accelerometer signal and the photoelectric encoder signal to obtain accurate angular velocity and angular acceleration information, which is used based on the model dynamic equation. The article also expounds on how to calibrate the installed accelerometer. The experiment and analysis of the interaction process between the robot and the external environment are carried out. The following conclusions are obtained: the momentum observer is essentially the same as the RTOB, the external torque estimation result has a large delay, the output result has a narrow bandwidth, and the sensitivity and accuracy of the external force estimation are both relatively poor. However, under the premise that the acceleration signal can be obtained accurately, the direct external force estimation method based on model dynamics has no delay. The output result can have higher bandwidth and has an accurate and sensitive external force estimation result. The external force estimation results, in turn, verify the effectiveness and accuracy of the accelerometer calibration algorithm and the EKF algorithm that integrates the accelerometer signal and the photoelectric encoder signal.

References:

[1] Li, J.; Li, S.Q.; Tian, G.H.; Shang, H.C. Muscle tension training method for series elastic actuator (SEA) based on gain-scheduled method. *Robotics and Autonomous Systems.* **2019**, *121*.

[2] Refour, E.M.; Sebastian, B.; Chauhan, R.J.; Ben-Tzvi, P. A General Purpose Robotic Hand Exoskeleton With Series Elastic Actuation. *ASME.J.Mechanisms Robotics.* **2019**, *11*.

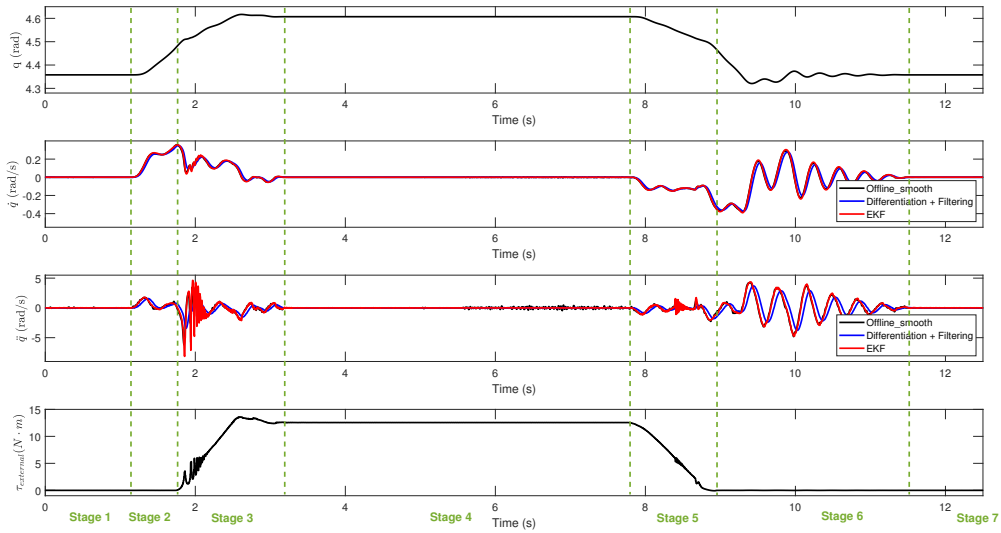


Fig. 4. Link states in different stages of system motion

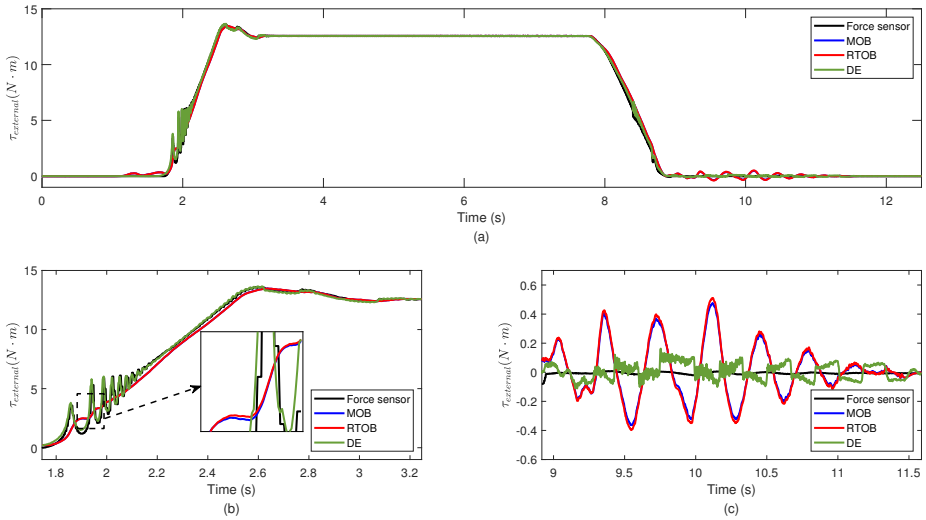


Fig. 5. The result of external torque estimation

[3] Vantilt, J.; Tanghe, K.; Afschrift, M. et al. Model-based control for exoskeletons with series elastic actuators evaluated on sit-to-stand movements.*J NeuroEngineering Rehabil.* **2019**, *16*.

[4] Zhang, S.; Zhu, Q.; Wu, J.; Xiong, R.; Gu, Y. Design and Compliance Control of Rehabilitation Exoskeleton for Elbow Joint Anchylosis. *2020 IEEE/ASME International Conference on Advanced Intelligent Mechatronics (AIM).* **2020**, 1896–1901.

[5] De Luca, A.; Mattone, R. Actuator failure detection and isolation using generalized momenta. *Proceedings of the 2003 IEEE International Conference on Robotics and Automation.* **2003**, 634–639.

[6] Wahrburg, A.; Morara, E.; Cesari, G.; Matthias, B.; Ding, H. Cartesian contact force estimation for robotic manipulators using Kalman filters and the generalized momentum. *2015 IEEE International Conference on Automation Science and Engineering (CASE).* **2015**, 1230–1235.

[7] Wahrburg, A.; Bös, J.; Listmann, K.D.; Dai, F.; Matthias, B.; Ding, H. Motor-Current-Based Estimation of Cartesian Contact Forces and Torques for Robotic Manipulators and Its Application to Force Control. *IEEE Transactions on Automation Science and Engineering.* **2018**, *15* 879–886.

[8] Suzuki, J.; Murakami, T.; Ohnishi, K. Position and force control of flexible manipulator with position sensitive device. *7th International Workshop on Advanced Motion Control.* **2002**, 414–419.

[9] Sariyildiz, E.; Ohnishi, K. An Adaptive Reaction Force Observer Design. *IEEE/ASME Transactions on Mechatronics.* **2015**, *20*, 750–760.

[10] Cardou, P.; Fournier, G.; Gagnon, P. A Nonlinear Program for Angular-Velocity Estimation From Centripetal-Acceleration Measurements. *IEEE/ASME Transactions on Mechatronics.* **2011**, *16*, 932–944.

[11] Vihonen, J.; Honkakorpi, J.; Mattila, J.; Visa, A. Geometry-aided inversion of manipulator telescopic link length from MEMS accelerometer and rate gyro readings. *2014 IEEE International Conference on Robotics and Automation (ICRA).* **2014**, 181–186.

[12] Vihonen, J.; Honkakorpi, J.; Koivumäki, J.; Mattila J.; Visa, A. Geometry-aided low-noise angular velocity sensing of rigid-body manipulator using MEMS rate gyros and linear accelerometers. *2014 IEEE/ASME International Conference on Advanced Intelligent Mechatronics.* **2014**, 570–575.